NANO LETTERS

2003
Vol. 3, No. 10
1341−1346

# Tethered Nano Building Blocks: Toward a Conceptual Framework for Nanoparticle Self-Assembly

**Zhenli Zhang,[†] Mark A. Horsch,[†] Monica H. Lamm,[†,‡] and Sharon C. Glotzer*[,†,§]**

*Departments of Chemical Engineering and Materials Science & Engineering, University of Michigan, Ann Arbor, Michigan 48109-2136*

*Received June 27, 2003; Revised Manuscript Received August 8, 2003*

**ABSTRACT**

**We perform molecular simulations to study the self-assembly of nanoparticles functionalized with oligomeric tethers attached to specific locations on the nanoparticle surface. We demonstrate that for certain categories of tethered nano building blocks the obtained morphologies may be predicted using concepts from block copolymer microphase separation and liquid-crystal phase ordering, whereas for other categories the unique packing constraints introduced by nanoparticle geometry and by nanoparticle–tether topology lead to structures far richer than those found in conventional block copolymer, surfactant, and liquid-crystal systems. Our results suggest the potential usefulness of considering tethered nano building blocks as a new class of "macromolecule" for assembling novel materials on the nanoscale.**

An impressive variety of nano building blocks, including nanospheres,[1] nanorods,[2] nanocubes,[3] nanoplates,[4,5] nanotetrapods,[6] and nanoprisms,[7] exists and continues to grow with breakthroughs in synthesis techniques. The application of nanotechnology to areas such as photonics and electronics, chemical and biological sensors, energy storage, and catalysis requires the manipulation of these nano-objects into functional materials and devices, and this remains a fundamental challenge. Self-assembly[8,9] is generally regarded as the most promising means for designing and controlling the bottom-up assembly of nanometer-scale objects into structures such as sheets, tubes, wires, and shells needed as scaffolds and structures for catalysis, hydrogen storage, nanoelectronic devices, and drug delivery. Although many nanoparticle assembly demonstrations have appeared in the literature,[10−19] few approaches offer a comprehensive, predictable, and generally applicable scheme. Increasingly, synthetic chemists are turning their attention to the functionalization of nano building blocks (both nanocrystals and supramolecular entities) with flexible oligomeric,[18,20−24] polymeric,[25−28] and biomolecular[17,29] tethers with specific and nonspecific interactions to direct their assembly. Although synthetic techniques to this point have not demonstrated ultimate control over the placement of these tethers, impressive progress has been made, and it is not unreasonable to suppose that an effective means for the precise positioning of tethers on the surfaces of nanoparticles of arbitrary geometry and composition may one day be achieved.[30]

From that viewpoint, it is useful to consider tethered nano building blocks as a new class of "macromolecule" with which to control nanoparticle assembly for new nanomaterials. Figure 1 shows a selection of possible topologies for tethered nano building blocks, arranged according to nanoparticle shape. Some of the topologies shown are reminiscent of tethered supramolecular entities such as dendrons,[28,31] silica cubes,[25,32] and fullerenes[27] reported in the literature, but other topologies have yet to be synthesized. Broadly speaking, tethered nano building blocks share features in common with block copolymers and surfactants, and we expect the appearance of ordered microphases to be governed by similar physics, whereby two or more incompatible species seek to minimize their free energy by aggregating with species of their own kind, subject to the topological constraint of being covalently linked to the incompatible species.[33] They also share features in common with liquid crystals, where molecular rigidity and shape can result in complex, ordered packings, including nematic, discotic, cholesteric, and other phases.[5,34]

We therefore seek to develop an intuitive framework for predicting the assembly of tethered nano building blocks akin to frameworks used to describe block copolymer[33] and surfactant[35,36] microphase separation and liquid-crystal phase ordering.[5,37] In this regard, molecular simulation of model nano building blocks can yield insight into the conditions under which various structures may be achieved, provided appropriate models can be devised and the length and time

* Corresponding author. E-mail: sglotzer@umich.edu.
[†] Department of Chemical Engineering.
[‡] New address: Department of Chemical Engineering, Iowa State University, Ames, Iowa 50011-2230.
[§] Department of Materials Science & Engineering.

10.1021/nl034454g CCC: $25.00 
**Published on Web 09/23/2003**

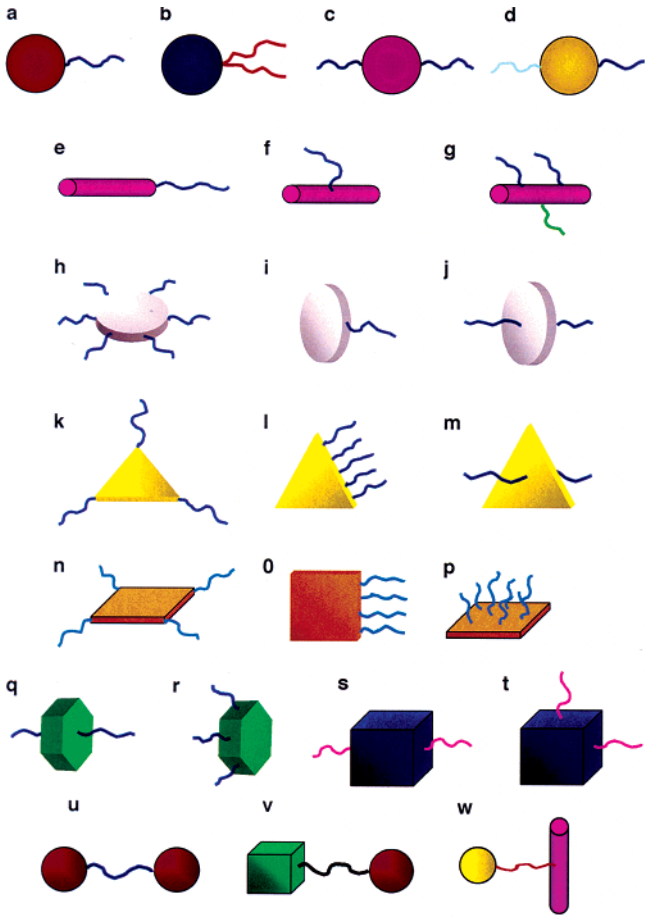


**Figure 1.** Representative tethered nano building blocks. (a−d) Tethered nanospheres. (e−g) Tethered nanorod. (h−p) Tethered nanoplate, including circular, triangular, and rectangular plates. (q, r) Tethered nanowheel. (s, t) Tethered nanocube. (u−w) Triblock nano building blocks created by joining two nano-objects with a polymer tether. All of the nanoparticle geometries depicted here have been synthesized.[2−5,7] The tethered topologies shown in a,[28] b,[27] e,[26] f and g,[21,57] h,[31] u,[25,28] and v[20] have been synthesized.

scales relevant to the assembly process can be efficiently accessed. As a first step, we use Langevin molecular dynamics (Brownian dynamics) simulations to study the self-assembly of minimal models of tethered nano building blocks. We show how tuning thermodynamic parameters and architectural features of the nano building blocks can control aspects of local and global ordering of the nanoparticles. We further demonstrate how, in some cases, the additional packing constraints introduced by the nanoparticle geometry[23,24,38] and the nano building block topology, combined with tether and nanoparticle immiscibility, lead to structures far richer than those known for conventional block copolymer, surfactant, and liquid-crystal systems.

Several simulation methods exist for studying assembly in block copolymers, liquid crystals, and other complex materials.[39] Brownian dynamics, a variant of molecular dynamics, is one method that is particularly well suited to studying the topological effects of nano building block geometries. Furthermore, as discussed below, Brownian dynamics allows for the implicit treatment of certain solvent

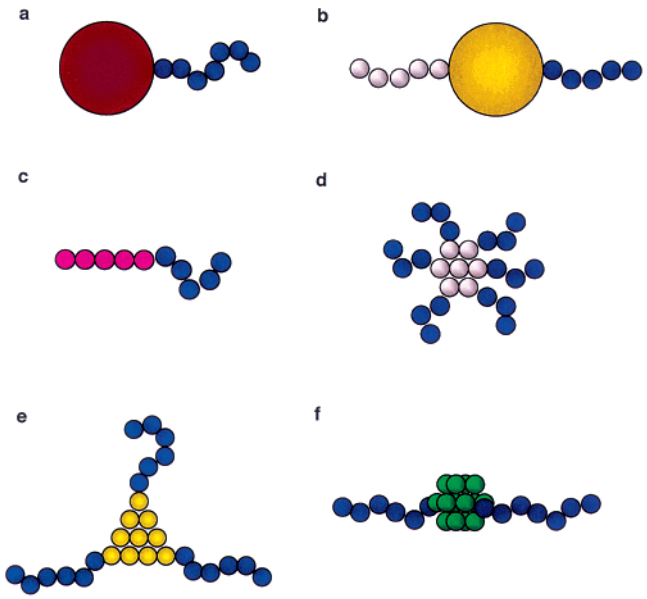


**Figure 2.** Model tethered building blocks studied in this work. Blue spheres represent monomers of the polymer tether. Large spheres represent nanospheres. Remaining spheres represent coarse-grained atoms frozen to create the desired nanoparticle. (a) Tethered nanosphere (Figure 1a). (b) Triblock polymer(A)−nanosphere−polymer(B) (Figure 1d). (c) Tethered nanorod (Figure 1e). (d) Tethered nanodisk (Figure 1h). (e) Tethered triangular nanoplate (Figure 1k). (f) Tethered nanowheel (Figure 1q).

effects; thus, the multiplicity of scales that must be bridged to simulate assembly in solution is achieved.

Figure 2 shows the set of model, tethered nano building blocks studied in this work. In the present paper, we consider tethered nanoparticles that realistically may contain hundreds to millions of atoms, depending on size and chemical composition. Because we seek to study the assembly of many such nanoparticles, it is computationally necessary to use a coarse-grained model in which groups of atoms within an individual nanoparticle or tether are represented by a single, coarse-grained "atom", thereby greatly reducing the overall number of forces that must be computed for each time step while retaining the roughness of the surface interactions expected in particles of nanoscopic dimension. Because we are interested in general trends rather than one specific system, we consider empirical pair potentials between "atoms" that capture the van der Waals-type interactions and excluded-volume interactions characteristic of many nanoparticle systems[24,29,40,41] and that have been successful in the study of phase separation and microphase separation of polymer blends, surfactants, and block copolymers.[35,42−44]

Our minimal model is as follows. For spherical nano objects, a nanoparticle is modeled as a single sphere of diameter $d$. Nonspherical nanoparticles are built by freezing $N_{np}$ spherical subunits ("atoms") of diameter $\sigma$, separated by distance $l_0 = 0.97\sigma$, into the desired nanoparticle geometry. A polymer tether is modeled as a bead-spring chain of $N_p$ monomers with diameter $\sigma$, where neighboring monomers along the chain are connected by a FENE potential[45,46] with average bond length $l_0$. Tethers are permanently connected to specific atoms on the nanoparticles

**Table 1**

| building block | morphology | volume fraction $\phi$ | reciprocal[e] temperature $\epsilon/kT$ | time step[e] $\Delta t(\epsilon/m\sigma^2)^{1/2}$ | simulation[e] time $t(\epsilon/m\sigma^2)^{1/2}$ |
|---|---|---|---|---|---|
| tethered nanosphere[a] | double layer | 0.24 | 4.0 | 0.01 | $7.7 \times 10^6$ |
| tethered nanosphere[b] | spherical | 0.24 | 4.0 | 0.01 | $1.8 \times 10^6$ |
| polymer(A)−nanosphere−polymer(B)[c] | lamellar | 0.57 | 1.0 | 0.01 | $10.0 \times 10^6$ |
| polymer(A)−nanosphere−polymer(B)[c] | cylindrical | 0.25 | 2.0 | 0.005 | $3.1 \times 10^6$ |
| polymer(A)−nanosphere−polymer(B)[c] | spherical | 0.21 | 2.0 | 0.01 | $2.2 \times 10^6$ |
| tethered nanorod[d] | lamellar | 0.44 | 1.0 | 0.01 | $3.0 \times 10^6$ |
| tethered nanowheel[a] | lamellar/sheets | 0.31 | 1.0 | 0.01 | $10.0 \times 10^6$ |
| tethered nanodisk[a] | columnar | 0.42 | 1.0 | 0.01 | $16.0 \times 10^6$ |
| tethered triangular nanoplate[a] | columnar | 0.31 | 1.2 | 0.01 | $12.0 \times 10^6$ |

[a] Solvent poor for nanoparticle and good for tethers. [b] Solvent good for nanospheres and poor for tethers. [c] Solvent good for A-type tethers and poor for nanospheres and B-type tethers. [d] Solvent neutral for nanorods and tethers. [e] Real units can be obtained by choosing a system temperature and values for the monomer mass and diameter.

via a FENE potential. This minimal model captures the essential, gross features of tethered nanoparticle topology. For specific systems, it is straightforward to incorporate more detailed interaction potentials parametrized by experimental values or informed by ab initio computations at the expense of substantially longer simulation times.

In neutral solvent, atoms or monomers of the same type interact with a 12−6 Lennard-Jones (LJ) potential, accounting for both excluded volume and van der Waals interactions.[47] The LJ potential is shifted and truncated at $2.5\sigma$ in the usual manner. For spherical nanoparticles modeled by a single atom of diameter $d > \sigma$, the interaction distance is measured from the surface of the nanoparticle. Monomers or atoms of different types interact with a purely repulsive Weeks−Chandler−Andersen soft-sphere potential,[48] accounting for excluded volume interactions. The selectivity of the solvent for different species is modeled by describing interactions between the favored species (good solvent) via a purely excluded volume interaction and those between the unfavored species (poor solvent) via a Lennard-Jones interaction.[49,50] The unfavored species (either tethers or nanoparticles) will then aggregate at low temperature. The degree of immiscibility and solvent quality is determined by the reciprocal temperature, $\epsilon/k_BT$, where $\epsilon$ is the potential well depth, $k_B$ is Boltzmann's constant, and $T$ is temperature.

In the Brownian dynamics method, each atom or monomer is subjected to conservative, frictional, and random forces $\mathbf{F}_i^C$, $\mathbf{F}_i^F$, and $\mathbf{F}_i^R$, respectively, and obeys the following equation of motion:[47]

$$m\ddot{\mathbf{r}}_i = \mathbf{F}_i^C + \mathbf{F}_i^F + \mathbf{F}_i^R \tag{1}$$

where $m$ is the atom's mass. Excluded volume, van der Waals, and bonding interactions are explicitly included in $\mathbf{F}_i^C$. Hydrodynamic drag, including size and shape effects, is included through the frictional force, which for individual atoms is $\mathbf{F}_i^F = -\gamma_i\mathbf{v}_i = -6\pi a\eta\mathbf{v}_i$, where $\gamma_i$ is the friction coefficient, $a$ is the atom's diameter, $\eta$ is the solvent viscosity, and $\mathbf{v}_i$ is the atom's velocity.[51] The Brownian motion of the nano building block resulting from the random bombardment of solvent molecules is included through $\mathbf{F}_i^R$ and can be calculated using the fluctuation dissipation theorem[44]

$$\langle \mathbf{F}_i^R(t)\, \mathbf{F}_j^R(t')\rangle = 6k_BT\gamma_i\,\delta_{ij}\delta(t-t') \tag{2}$$

At every time step, frozen subunits move together as a rigid object using the method of quaternions.[47]

Each of the simulations is carried out at a fixed volume fraction $\phi = NV_0/V$ of nano building blocks in a cubic simulation box to which periodic boundaries are applied, where $N$ is the total number of atoms and monomers, $V_0 = \pi\sigma^3/6$ is the volume of an individual atom or monomer, and $V$ is the total system volume. The system sizes are large enough to avoid finite size effects in the local structure and small enough to achieve equilibration in a reasonable amount of time.[52] In all cases, systems are initially equilibrated at effectively infinite temperature ($\epsilon/k_BT = 0$) until they are disordered. The temperature is then instantaneously reduced to the target temperature ($\epsilon/k_BT \approx 1.0-4.0$) and run at this temperature until an equilibrium structure is obtained. To avoid local energy minima, cooling is performed for several different initial configurations. The volume fraction and target reciprocal temperature are selected to produce a specific morphology and are chosen on the basis of known morphologies arising from microphase separation of simple diblock copolymers in selective solvent.[35] (See Table 1 for details of each simulation.)

To illustrate the influence of solvent selectivity on the assembled structure, Figure 3, a−d, shows results from simulations of tethered nanospheres (Figure 1a). Figure 3a shows a lamellar structure formed in a solvent poor for nanospheres and good for tethers. If no tethers were present, then the nanospheres (again in poor solvent) would form a compact 3-D cluster in an effort to minimize contact with the solvent. Instead, the nanospheres pack in a 2-D hexagonal array and form double layers (Figure 3b) to maximize contact and satisfy excluded volume interactions among tethers. Figure 3c and d shows how reversing the solvent selectivity to be good for nanospheres and poor for tethers induces the formation of spherical micelles, where tethers cluster to avoid contact with the solvent, causing the nanospheres to form spherical shells instead of double layers.

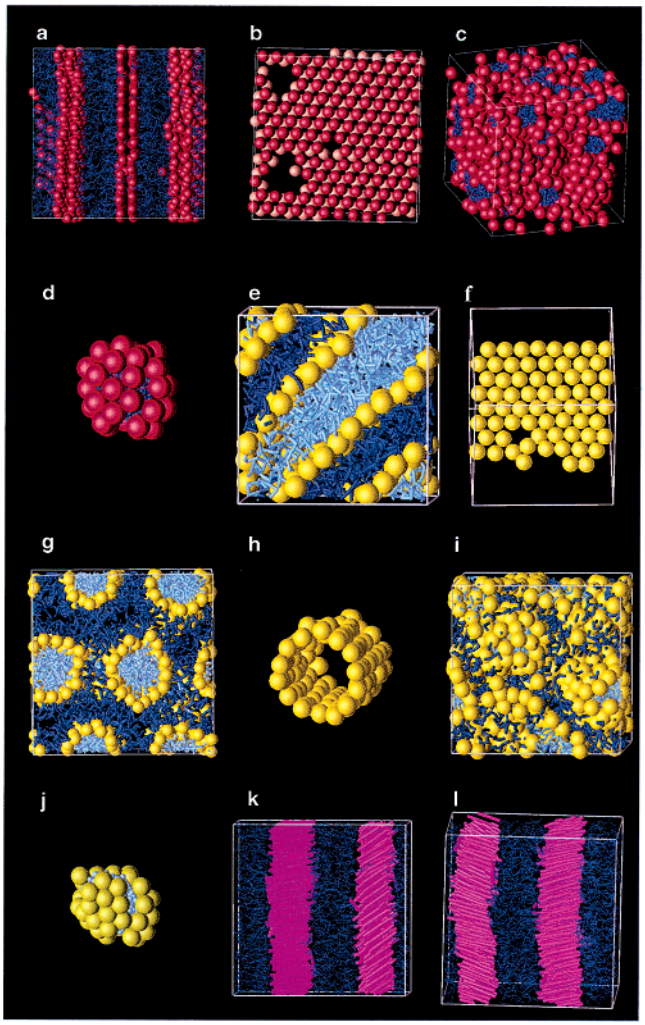


**Figure 3.** Equilibrium structures formed by tethered nanosphere and nanorod building blocks. **(**a) Lamellar phase formed by 800 tethered nanospheres (Figure 1a) with tethers of length $N_p = 7$ attached to spheres of diameter $d \approx 3\sigma$ in a solvent good for tethers and poor for nanospheres. (b) Face view of a nanosphere double layer (spheres in second layer colored light red, tethers removed for clarity) from a. (c) Tethered nanospheres in a form a spherical micelle phase when placed in a solvent poor for the tethers and good for the nanospheres. (d) Single spherical micelle from c. (e) Lamellar phase formed by 200 triblock polymer(A)−nanosphere−polymer(B) building blocks (Figure 1d) with nanospheres of diameter $d \approx 2\sigma$ and tethers of length $N_p = 5$. A-type tethers are white; B-type tethers are blue. (f) Face view of a single monolayer composed of nanospheres from e (tethers removed for clarity). (g) Cylindrical phase formed by 800 polymer(A)−nanosphere−polymer(B) building blocks. (h) Single cylinder from g (tethers removed for clarity). (i) Spherical micelle phase formed by 800 polymer(A)−nanosphere−polymer(B) building blocks. (j) Single spherical micelle from i (blue tethers removed for clarity). (k) Lamellar phase with tilt angle $\theta = 33°$ formed by 800 tethered nanorods (Figure 1e) in a neutral solvent. Rods of length $N_{np} = 5$ frozen subunits are attached to tethers of length $N_p = 6$ monomers. (l) Lamellar phase with tilt angle $\theta = 16°$ formed by tethered nanorods with $N_p = 5$.

To demonstrate control over morphology based on the concentration of tethered building blocks in solution, Figure 3, e−j, shows equilibrium structures obtained with "triblock reminiscent" polymer(A)−nanosphere−polymer(B) building blocks (Figure 1d) in a solvent poor for nanospheres and A-type tethers and good for B-type tethers. Figure 3, e and f, shows a lamellar structure where the nanospheres form 2-D hexagonally arranged monolayers. By lowering the concentration and the target temperature, we obtain cylindrical (Figure 3, g and h) and spherical micelle (Figure 3, i and j) phases, where nanospheres pack as cylindrical or spherical shells, respectively, with A-type tethers in the shell interior. The influence of concentration and temperature on the equilibrium morphology for this building block is qualitatively consistent with the phase behavior of a typical block copolymer in solution.[35]

Control over structure can also be obtained by varying the relative concentration of each component. Figure 3, k and l, shows equilibrium lamellar structures formed by tethered nanorods (Figure 1e) in a neutral solvent. The rods pack in layers, oriented with a tilt angle, $\theta$, with respect to the normal direction of the lamellar interface. Here, $\theta$ increases from 16° to 33° by increasing the tether length from five to six monomers (i.e., increasing the relative volume fraction of tether). The tilt angle arises for entropic reasons due to the excluded volume interactions among tethers,[53] and its dependence on the relative block length has been predicted[53] and observed in rod-coil block copolymers[54] where the "rod" block is a rodlike polymer chain or liquid crystal. Here, the nanorod could represent an inorganic particle[2,22,23,55] or a short carbon nanotube.[26] We emphasize that all equilibrium morphologies presented here are obtained without a priori knowledge of their structure by instantaneously cooling initially disordered systems to a temperature at which tethers and nanoparticles are immiscible.

The above examples demonstrate that intuition from block copolymer and liquid-crystal phase ordering is useful for predicting the self-assembly of tethered nano building blocks. Next, we explore morphologies predicted with a few of the more exotic shapes shown in Figure 1. Figure 4, a and b, shows equilibrium columnar structures formed by tethered nanodisks (Figure 1h) in a solvent poor for disks and good for tethers. Here, six tethers are attached equidistantly along the edge of a disk so that attractive interactions between the disks lead to face-to-face stacking. The columns arrange in a hexagonal pattern in the plane orthogonal to the columnar axis to maximize contact while satisfying excluded volume interactions among tethers. These columnar structures are reminiscent of those observed in discotic liquid crystals[56] and have recently been observed to form using oligomerically stabilized platelet particles.[24] Here, the spacing between columns and stacking within columns is controlled by tether length and rigidity. Moreover, disks in each column have a tilt angle with respect to the interface normal direction driven by excluded volume interactions between tethers as in the tethered nanorod system described above. Figure 4, c and d, shows hexagonally arranged columnar structures formed by tethered triangular plates (Figure 1k) in a solvent poor for triangles and good for tethers. Here, triangular plates in each column form twisted structures. These twisted structures again arise from the competition between the attraction among nanoparticles and the excluded volume interactions among tethers on neighboring plates. We anticipate that the

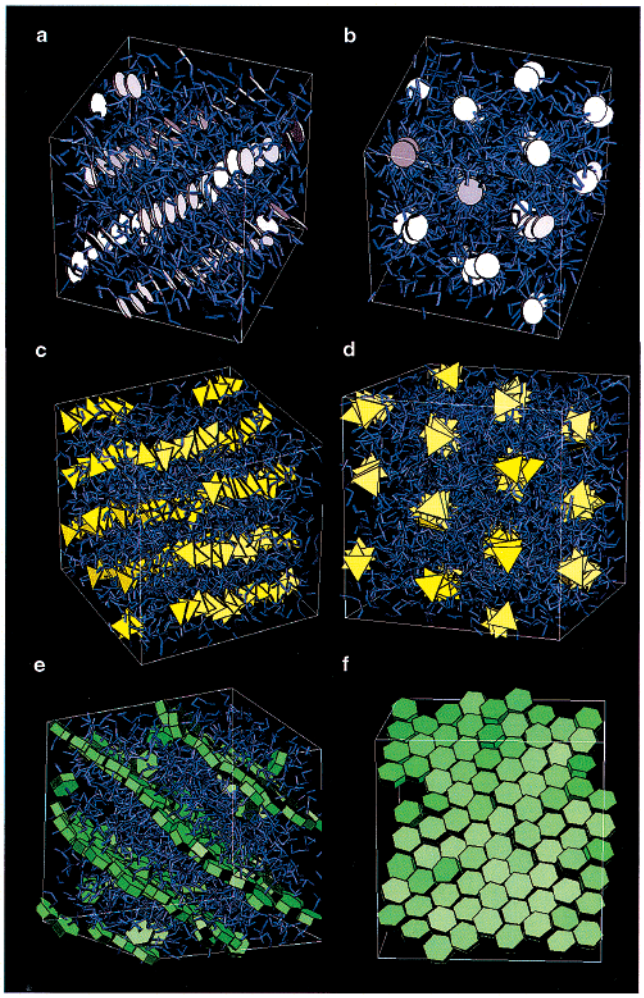


**Figure 4.** Equilibrium structures formed by tethered nanoplate and nanowheel building blocks. (a) Hexagonally packed columnar phase formed by 120 tethered nanodisks (Figure 1h). Six tethers of length $N_p = 3$ are attached to disks with $N_{np} = 7$. (b) Face view of the columnar phase in a. (c) Hexagonally packed columnar phase formed by 200 tethered triangular nanoplates (Figure 1k). Three tethers of length $N_p = 6$ are attached to triangular plates with $N_{np} = 10$. (d) Face view of the columnar phase in c. (e) Lamellar phase of sheetlike structure formed by 200 tethered nanowheels (Figure 1q) with polymer tethers of length $N_p = 7$ attached to the faces of cylinders with $N_{np} = 14$. (f) Monolayer sheet of nanowheels (tethers removed for clarity).

twist angle may be controlled by adjusting the length of the tethers relative to the size of the triangular plates. Finally, Figure 4, e and f, shows layered, sheetlike structures obtained with tethered "nanowheels", where tethers are attached on opposite faces of the wheels, preventing the wheels from stacking face-to-face (Figure 1q). The solvent is poor for nanowheels and good for tethers. Sheets form to maximize contact among the nanowheels while satisfying excluded volume interactions among tethers. Within the sheets, nanowheels pack edge-to-edge in hexagonal arrays because of the geometry of the nanoparticle. Recent experimental discoveries of stable sheets of in 2-(dimethylamino)ethanethiol(DMAET)-stabilized CdTe nanoparticles may potentially be explained via a similar mechanism.[41]

The simulation results presented here predict that by tethering oligomers to specific locations on nanoparticle surfaces the thermodynamically driven immiscibility of tethers and nanoparticles can be used to facilitate the self-assembly of nanoparticles into specific structures that are potentially far richer than those known for conventional block copolymer, surfactant, and liquid-crystal systems because of the complex geometry and topology of the tethered nanoparticles. This strategy should prove successful in device fabrication where novel conducting pathways (e.g., nanoshells in Figure 3, c, g, and i, or nanosheets in Figure 3, a, e, and k, and nanowires in Figure 4, a and b) could be created through an insulating material. We demonstrated that local nanoparticle alignment and spacing can be controlled by variations in tether length (and presumably, stiffness), which may be used to tune the optical and electronic properties of self-assembled materials. For example, changing the twist in a nanowire composed of triangular plate nanoparticles allows for control over the contact area and, ultimately, current flow. Although many demonstrations of functionalized nano building blocks exist in the literature,[17−28,32,57] many of the tethered building blocks presented here have yet to be synthesized. The diversity of structures demonstrated in this work—mono- and double-layer sheets, solid cylinders or wires, and cylindrical and spherical nanoshells—should provide substantial motivation for attempting their synthesis. In parallel with such efforts, simulations of the type described here can be used to map out phase diagrams systematically for general classes of model nano building blocks as a guide toward how one might directly engineer the self-assembly of specific assembled structures. Here, we used relatively simple interaction potentials to describe nanoparticle and tether immiscibility in solvent in the interest of constructing a general model that can be studied for large collections of nano building blocks with reasonable computing power. Comparison with specific experimental systems can be carried out by parametrizing nanoparticle−tether interactions using experimental data or, for some systems, ab initio computations. Efforts in this direction are underway.

**Acknowledgment.** Financial support was provided by the Department of Energy, grant no. DE-FG02-02ER46000. We thank the National Partnership for Advanced Computational Infrastructure (NPACI) and the University of Michigan Center for Advanced Computing for a generous allocation of CPU time on the AMD-Athlon cluster. We are grateful to J. Kieffer, N. Kotov, and M. J. Solomon for helpful comments on the manuscript.

## References

(1) Murray, C. B.; Kagan, C. R.; Bawendi, M. G. *Annu. Rev. Mater. Sci.* **2000**, *30*, 545−610.
(2) Busbee, B. D.; Obare, S. O.; Murphy, C. J. *Adv. Mater.* **2003**, *15*, 414−416.
(3) Sun, Y. G.; Xia, Y. N. *Science* **2002**, *298*, 2176−2179.
(4) Pinna, N.; Weiss, K.; Urban, J.; Pileni, M.-P. *Adv. Mater.* **2001**, *13*, 261−264.
(5) Kooij, F. M. V. d.; Kassapidou, K.; Lekkerkerker, H. N. W. *Nature* **2000**, *406*, 868−871.
(6) Manna, L.; Milliron, D. J.; Meisel, A.; Scher, E. C.; Alivisatos, A. P. *Nat. Mater.* **2003**, *2*, 382.
(7) Jin, R. C.; Cao, Y. W.; Mirkin, C. A.; Kelly, K. L.; Schatz, G. C.; Zheng, J. G. *Science* **2001**, *294*, 1901−1903.
(8) Whitesides, G. M.; Grzybowski, B. *Science* **2002**, *295*, 2418−2421.

(9) Kamien, R. D. *Science* **2003**, *299*, 1671−1673.
(10) Stupp, S. I.; Braun, P. V. *Science* **1997**, *277*, 1242−1248.
(11) Templin, M.; Franck, A.; Chesne, A. D.; Leist, H.; Zhang, Y. M.; Ulrich, R.; Schadler, V.; Wiesner, U. *Science* **1997**, *278*, 1795−1798.
(12) Lopes, W. A.; Jaeger, H. M. *Nature* **2001**, *414*, 735−738.
(13) Gauffre, F.; Roux, D. *Langmuir* **1999**, *15*, 3738−3747.
(14) Mamedov, A. A.; Belov, A.; Giersig, M.; Mamedova, N. N.; Kotov, N. A. *J. Am. Chem. Soc.* **2001**, *123*, 7738−7739.
(15) Pileni, M. P. *J. Phys. Chem. B* **2001**, *105*, 3358−3371.
(16) Davis, S. A.; Breulman, M.; Rhodes, K. H.; Zhang, B. J.; Mann, S. *Chem. Mater.* **2001**, *13*, 3218−3226.
(17) Parak, W. J.; Pellegrino, T.; Micheel, C. M.; Gerion, D.; Williams, S. C.; Alivisatos, A. P. *Nano Lett.* **2003**, *3*, 33−36.
(18) Boal, A. K.; Ilhan, F.; DeRouchey, J. E.; Thurn-Albrecht, T.; Russell, T. P.; Rotello, V. M. *Nature* **2000**, *404*, 746−748.
(19) Niemeyer, C. M. *Curr. Opin. Chem. Biol* **2000**, *4*, 609−618.
(20) Carroll, J. B.; Frankamp, B. L.; Rotello, V. M. *Chem. Commun.* **2002**, 1892−1893.
(21) Saini, R. K.; Chiang, I. W.; Peng, H. Q.; Smalley, R. E.; Billups, W. E.; Hauge, R. H.; Margrave, J. L. *J. Am. Chem. Soc.* **2003**, *125*, 3617−3621.
(22) Puntes, V. F.; Krishnan, K. M.; Alivisatos, A. P. *Science* **2001**, *291*, 2115−2117.
(23) Korgel, B. A.; Fitzmaurice, D. *Adv. Mater.* **1998**, *10*, 661−665.
(24) Viau, G.; Brayner, R.; Poul, L.; Chakroune, N.; Lacaze, E.; Fievet-Vincent, F.; Fievet, F. *Chem. Mater.* **2003**, *15*, 486-494.
(25) Kim, B. S.; Mather, P. T. *Macromolecules* **2002**, *35*, 8378−8384.
(26) Riggs, J. E.; Guo, Z. X.; Carroll, D. L.; Sun, Y. P. *J. Am. Chem. Soc.* **2000**, *122*, 5879−5880.
(27) Song, T.; Dai, S.; Tam, K. C.; Lee, S. Y.; Goh, S. H. *Polymer* **2003**, *44*, 2529−2536.
(28) Song, T.; Dai, S.; Tam, K. C.; Lee, S. Y.; Goh, S. H. *Langmuir* **2003**, *19*, 4798−4803.
(29) Mirkin, C. A.; Letsinger, R. L.; Mucic, R. C.; Storhoff, J. J. *Nature* **1996**, *382*, 607−609.
(30) Murphy, C. J. *Science* **2002**, *298*, 2139.
(31) Ungar, G.; Liu, Y. S.; Zeng, X. B.; Percec, V.; Cho, W. D. *Science* **2003**, *299*, 1208−1211.
(32) Pyun, J.; Matyjaszewski, K.; Wu, J.; Kim, G.-M.; Chun, S. B.; Mather, P. T. *Polymer* **2003**, *44*, 2739−2750.
(33) Bates, F. S.; Fredrickson, G. H. *Phys. Today* **1999**, *52*, 32−38.
(34) Percec, V.; Glodde, M.; Bera, T. K.; Miura, Y.; Shiyanovskaya, I.; Singer, K. D.; Balagurusamy, V. S. K.; Heiney, P. A.; Schnell, I.; Rapp, A.; Spiess, H. W.; Hudson, S. D.; Duan, H. *Nature* **2002**, *419*, 384−387.
(35) Larson, R. G. *J. Phys. II* **1996**, *6*, 1441−1463.
(36) Holmqvist, P.; Alexandridis, P.; Lindman, B. *Macromolecules* **1997**, *30*, 6788−6797.
(37) Cao, W. Y.; Munoz, A.; Palffy-Muhoray, P.; Taheri, B. *Nat. Mater.* **2002**, *1*, 111−113.
(38) Tsonchev, S.; Schatz, G. C.; Ratner, M. A. *Nano Lett.* **2003**, *3*, 623−626.
(39) Glotzer, S. C.; Paul, W. *Annu. Rev. Mater. Res.* **2002**, *32*, 401−436.
(40) Caruso R. A.; Antonietti, M. *Chem. Mater.* **2001**, *13*, 3272−3282.
(41) Kotov, N.; Tang, Z.; Wang, L. To be submitted for publication.
(42) Padilla, P.; Toxvaerd, S. *J. Chem. Phys.* **1997**, *106*, 2342−2347.
(43) Laradji, M.; Toxvaerd, S.; Mouritsen, O. G. *Phys. Rev. Lett.* **1996**, *77*, 2253−2256.
(44) Grest, G. S.; Lacasse, M.-D. *J. Chem. Phys.* **1996**, *105*, 10583−10594.
(45) Grest, G. S.; Kremer, K. *Phys. Rev. A* **1986**, *33*, 3628−3631.
(46) Rudisill, J. W.; Cummings, P. T. *Rheol. Acta* **1991**, *30*, 33−43.
(47) Allen, M. P.; Tildesley, D. J. *Computer Simulation of Liquids*; Clarendon: Oxford, U.K., 1987.
(48) Weeks, J. D.; Chandler, D.; Andersen, H. C. *J. Chem. Phys.* **1971**, *54*, 5237−.
(49) Kim, S. H.; Jo, W. H. *Macromolecules* **2001**, *34*, 7210−7218.
(50) Ding, J.; Carver, T. J.; Windle, A. H. *Comput. Theor. Polym. Sci.* **2001**, *11*, 483−490.
(51) Note that the only hydrodynamic effect included is the drag force and that any spatially or temporally correlated motion of solvent molecules is neglected. It can be argued that because the simulations are performed at relatively high volume fractions (Table 1) hydrodynamic effects are subtle compared to the conservative forces.
(52) For example, the system shown in Figure 3g contains 8800 “atoms” and monomers and required roughly 300 CPU hours per AMD-Athlon 1800 processor to assemble into the morphology shown.
(53) Halperin, A. *Macromolecules* **1990**, *23*, 2724−2731.
(54) Chen, J. T.; Thomas, E. L.; Ober, C. K.; Hwang, S. S. *Macromolecules* **1995**, *28*, 1688−1697.
(55) Jana, N. R.; Gearheart, L.; Murphy, C. J. *Chem. Commun.* **2001**, 617−618.
(56) Chaikin, P. M.; Lubensky, T. C. *Principles of Condensed Matter Physics*, 2nd ed.; Cambridge University Press: New York, 1997.
(57) Boul, P. J.; Liu, J.; Mickelson, E. T.; Huffman, C. B.; Ericson, L. M.; Chiang, I. W.; Smith, K. A.; Colbert, D. T.; Hauge, R. H.; Margrave, J. L.; Smalley, R. E. *Chem. Phys. Lett.* **1999**, *310*, 367−372.

NL034454G